

# METROPOLITAN MANILA SEISMIC HAZARD MAP USING MIDORIKAWA & HORI SITE AMPLIFICATION MODEL

\*Jonathan R. Dungca<sup>1</sup> and Mariamae Francia G. Montejo<sup>2</sup>

<sup>1</sup>Faculty, De La Salle University, Philippines; <sup>2</sup>Graduate Student, De La Salle University, Philippines

\*Corresponding Author, Received: 30 Nov. 2021, Revised: 01 Feb. 2022, Accepted: 23 Feb. 2022

**ABSTRACT:** Since Metropolitan Manila is known to be susceptible to seismic hazards, it is necessary to consider multiple factors in assessing this hazard. Aside from ground motion, the properties of soil which lead to the amplification of seismic waves should be considered. This study aimed to develop a seismic hazard map for Metro Manila considering the soil properties in the area by using Midorikawa & Hori site amplification model. Probabilistic seismic hazard assessment was conducted using earthquake data within 250 km of Metropolitan Manila for 10% and 2% probabilities of exceedance. The site amplification factors were computed using calculated shear wave velocities from SPT-N values. The calculated ground motions were amplified using the site amplification factors considering short-period and mid-period amplifications. The constructed maps of amplified peak ground acceleration (PGA) values showed how soil properties affect the ground motion. It was found that for a short-period amplification, the average PGAs is 0.538 g, and 0.659 g for 10%, and 2% probabilities of exceedance, respectively. While for mid-period amplification, the average PGAs is 0.589 g, and 0.830 g for 10%, and 2% probabilities of exceedance. Using the amplified seismic hazard maps, a better approximation of seismic hazards can be generated for future use.

**Keywords:** *Site amplification, Shear wave velocity, Peak ground acceleration, Probabilistic seismic hazard assessment, Metro Manila*

## 1. INTRODUCTION

Since the Philippines is situated within the Pacific Ring of Fire, the country is considered highly vulnerable to natural hazards such as earthquakes. Typically the damage caused by earthquakes is defined by the magnitude of the event and the distance from the site to the source. However, it is also necessary to consider the varying geological conditions in the area as it also affects the hazards caused by earthquakes [1].

Site amplification refers to the amplification of the earthquake waves as they travel from the source through the soil due to the local geological conditions in the site which is often characterized by shear wave velocity ( $V_s$ ) [2]. Unlike the studies for liquefaction and slope stability, only a few research in the country have been conducted which consider the effect of site amplification on earthquake hazards due to a general shortage of data for soil profiles and shear wave velocities. Since Metropolitan Manila or Metro Manila is regarded to be susceptible to earthquake hazards and site amplification due to its variable geology [3], it is necessary to include the effects of soil conditions in the evaluation to provide a more accurate representation of ground motion intensities.

In a previous study [4], a reference for site amplification of Metro Manila was developed, however, the site amplification model used in the study is only applicable to strains less than 1% and for periods that are less than or equal to 0.5 seconds.

With this, the study aims to develop seismic hazard maps considering site amplification of Metro Manila using a site amplification model [5] that is designed for higher strains and different periods, such as short-period and mid-period amplifications. The developed seismic hazard maps show the amplified peak ground accelerations in the study area for probabilities of exceedance of 10% and 2%. With the development of these amplified hazard maps, a reference and a basis are provided to determine how local site conditions affect ground motion intensities.

## 2. RESEARCH SIGNIFICANCE

Metro Manila, being the capital of the Philippines, has the densest population in the country and is considered a major contributor to the country's economy. This shows how important it is for the region to be prepared whenever disaster strikes, especially since its location and soil conditions make it even more vulnerable. By considering site amplification in evaluating hazards, the maps will be able to provide a more accurate representation of seismic hazards for future planning and assessments.

## 3. METHODOLOGY

The location of the study covers the area of Metro Manila. The region has a total of sixteen (16) cities and one (1) municipality. In this study, a

probabilistic seismic hazard assessment (PSHA) was conducted to determine the peak accelerations at bedrock ( $PA_{rock}$ ) within the study area. The site amplification factors were then identified using the average shear wave velocities ( $V_{S30}$ ) in Metro Manila and were used to amplify  $PA_{rock}$  and obtain the peak accelerations at the ground surface.

### 3.1 Probabilistic Seismic Hazard Assessment

In conducting PSHA, the equation of the probability theorem [6] is shown in Eq. (1). The equation shows the computation of the probability of exceeding a value of a ground motion parameter, considering the possible magnitudes or locations of an earthquake.

$$\lambda_{y^*} = \sum_{i=1}^{N_S} \sum_{j=1}^{N_M} \sum_{k=1}^{N_R} v_i P[Y > y^* | m_j, r_k] P[M = m_j] P[R = r_k] \quad (1)$$

where:

$\lambda_{y^*}$  = total mean annual exceedance rate for peak acceleration level  $y^*$ ;

$N_S$  = total number of potential earthquakes source in the study area;

$N_M$  = total number of magnitude intervals considered;

$N_R$  = total number of distance intervals considered;

$I$  = average rate of magnitude exceedance for source  $i$ ;

$P[Y > y^* | m_j, r_k]$  = probability that a ground motion parameter  $Y$  will exceed the peak acceleration level  $y^*$  at a specific magnitude interval  $m_j$  and a specific distance interval  $r_k$ ;

$P[M = m_j]$  = probability that a magnitude  $M$  will be included in the magnitude interval  $m_j$ ;

$P[R = r_k]$  = probability that a distance  $R$  will be included in the distance interval  $r_k$ .

In this study, the earthquake sources within 250 kilometers (km) of Metro Manila were considered and categorized as either linear sources or areal sources. For linear sources, the probability density function [6] for distance shown in Eq. (2) is used.

$$f_R(r) = \frac{r}{L_f \sqrt{r^2 - r_{min}^2}} \quad (2)$$

where:

$f_R(r)$  = probability density function for distance,  $R$ ;

$r$  = source-to-site distance;

$L_f$  = length of fault;

$I$  = shortest site-to-source distance.

For areal sources, the relation [7] was used as shown in Eq. (3). The area was further divided into square elements. Equation (2) was used to obtain the probability distribution considering the shortest distance from the center of each element to the site.

$$M = 4.532 + 0.887 \log A \quad (3)$$

where:

$A$  = rupture area;

$M$  = earthquake surface magnitude when  $L$  or  $W \leq 100$  km, in moment magnitude otherwise.

The probability distribution for magnitude was computed using the probability density function [6] shown in Eq. (4).

$$f_M(m) = \frac{\beta \exp[-\beta(m - m_0)]}{1 - \exp[-\beta(m_{max} - m_0)]} \quad (4)$$

where:

$f_M(m)$  = probability density function;

$m$  = mean magnitude within the range;

$m_0$  = minimum magnitude;

$m_{max}$  = maximum magnitude.

$\beta = 2.303b$ ;

$b$  = seismic constant.

In computing the probability distribution of the ground motion parameter exceedance, the ground motion prediction equations (GMPE) by [8] are shown in Eq. (5), Eq. (6), and Eq. (7) were used for shallow earthquakes. The GMPE by [9] shown in Eq. (8) and Eq. (9) were used for earthquakes generated by subduction zones.

$$\log y = -1.02 + 0.249M_w - \log r - 0.00255r \quad (5)$$

$$r = (R^2 + 7.3^2)^{1/2} \quad (6)$$

$$\sigma = 0.26 \quad (7)$$

where:

$y$  = peak horizontal acceleration on seismic bedrock;

$M_w$  = moment magnitude;

$r$  = nearest distance to rupture zone in km.

$$\ln y = 0.2418 + 1.414M_w + C_1 + C_2(10 - M_w)^3 + C_3 \ln(r + 1.7818e^{0.554M_w}) + 0.00670H + 0.3846Z_T \quad (8)$$

$$\sigma = C_4 + C_5M_w \quad (9)$$

where:

$y$  = spectral acceleration;

$C_n$  = regression coefficients [9];

$Z_T$  = source type indicator.

The value of  $P[Y > y^* | m_j, r_k]$  is computed using the equation by [6] shown in Eq. (10).

$$P[Y > y^* | m_j, r_k] = 1 - F_Y(y^*) \quad (10)$$

where:

$F_Y(y^*)$  = value of the cumulative distribution function (CDF) of  $Y$  at  $m$  and  $r$ .

The value of  $F_Y(y^*)$  is computed using the standard normal variate shown in Eq. (11).

$$z = \frac{\ln y^* - \ln Y}{\sigma} \quad (11)$$

where:

$z$  = Z-score corresponding to the ground motion parameter.

When the values of  $\lambda_{y^*}$  were computed considering the target accelerations from 0.05 g to 1.0 g, the seismic hazard curve was constructed by plotting the accelerations against the mean annual rate of exceedance. By combining the seismic hazard curve with the Poisson model shown in Eq. (12), the peak accelerations at bedrock ( $PA_{rock}$ ) for probabilities of exceedance of 10% and 2% in 50 years were computed.

$$P[Y_T > y^*] = 1 - e^{-\lambda_{y^*} T} \quad (12)$$

where:

$P[Y_T > y^*]$  = probability of exceedance of  $y^*$  in a time period of  $T$ .

### 3.2 Evaluation of Site Amplification

The average shear wave velocities ( $V_{S30}$ ) and the rock were used to quantify the site amplification. To calculate  $V_{S30}$ , the SPT-N data or RQD values from the borehole data in Metro Manila were gathered and processed.

For SPT-N values, the model by [10] is used to calculate  $V_s$  as shown in Eq. (13). For RQD values, interpolation is done using the table of values by [11] shown in Table 1.

$$V_s = 77.13N^{0.377} \quad (13)$$

where:

$N$  = raw standard penetration resistance.

After computing  $V_s$  for each soil layer, the  $V_{S30}$  for each site is computed. For soil data with depths greater than 30 meters, the equation by [12] in Eq. (14) was used, otherwise, an extrapolation shown in Eq. (15) was conducted as proposed by [13].

Table 1 Typical values of  $V_s$  for a given RQD [11]

RQD (%)	$V_s$ (m/s)
$0 < \text{RQD} \leq 50$	600
65	760
80	1500
90	2500
100	3400

$$V_{S30} = \frac{\sum_{i=1}^N h_i}{\sum_{i=1}^N \frac{h_i}{v_i}} \quad (14)$$

$$\log V_{S30} = c_0 + c_1 \log V_{SZ} + c_2 (\log V_{SZ})^2 \quad (15)$$

where:

$I$  = thickness of soil layers

$v_i$  = shear wave velocity at *layer* at the top 30 meters;

$V_{SZ}$  = average shear wave velocity at termination depth;

$c_n$  = regression coefficients [13].

The shear wave velocity map of Metro Manila was then constructed in mapping software using the computed  $V_{S30}$  values. The  $V_{S30}$  and  $PA_{rock}$  values were used to compute the site amplification factors using the model by [14] shown in Eq. (16).

$$\ln AF = a \ln V_{S30} + b \quad (16)$$

where:

$AF$  = amplification factor;

$a, b$  = regression coefficients in the function of  $PA_{rock}$ .

The regression coefficients [5] are computed depending on whether the amplification being considered is short-period amplification or mid-period amplification. Short-period amplification ( $F_a$ ) covers a period of 0.1 to 0.5 seconds, whose regression coefficients can be computed using Eq. (17) and Eq. (18).

$$a = 0.43PA_{rock}^2 + 0.79PA_{rock} - 0.71 \quad (17)$$

$$b = -3.04PA_{rock}^2 - 5.40PA_{rock} + 4.98 \quad (18)$$

Mid-period amplification ( $F_v$ ) covers a period of 0.4 to 2.0 seconds and its regression coefficients can be computed using Eq. (19) and Eq. (20).

$$a = 0.27PA_{rock}^2 + 0.07PA_{rock} - 0.72 \quad (19)$$

$$b = -1.51PA_{rock}^2 - 0.62PA_{rock} + 4.91 \quad (20)$$

The amplification factors were used to amplify

the peak acceleration values computed from the GMPEs, from which new seismic hazard curves were constructed. With this, the amplified peak ground acceleration (PGA) values are computed for 10% and 2% probabilities of exceedance.

#### 4. RESULTS AND DISCUSSION

In this study, earthquake data with a minimum magnitude of 4.0 and spanning from the years 1907 to 2020 were obtained from the Philippine Institute of Volcanology and Seismology (PHIVOLCS). The geotechnical data, on the other hand, were collected from past studies by [5], and [14-18].

##### 4.1 Seismic Hazard Maps

In developing the seismic hazard maps, a geographic information system (GIS) was used similar to [19]. A total of 17 active faults and 1695 earthquake events within 250 km of Metro Manila was considered.

Considering the probabilities of exceedance (POE) of 10% and 2%, the  $PA_{rock}$  values in Metro Manila were computed. Table 2 shows a summary of the rock values for each city in Metro Manila considering 10% and 2% POE.

Table 2 Average  $PA_{rock}$  values in Metro Manila per city and municipality

Location	rock (g)	
	10% POE	2% POE
Caloocan	0.390	0.581
Las Piñas	0.430	0.638
Makati	0.451	0.679
Malabon	0.324	0.480
Mandaluyong	0.456	0.687
Manila	0.383	0.571
Marikina	0.442	0.665
Muntinlupa	0.475	0.706
Navotas	0.296	0.437
Parañaque	0.448	0.669
Pasay	0.426	0.637
Pasig	0.443	0.666
Pateros	0.457	0.668
Quezon City	0.436	0.656
San Juan	0.452	0.682
Taguig	0.456	0.685
Valenzuela	0.337	0.500

As seen in Table 2, the average  $PA_{rock}$  values in Metro Manila vary from as low as 0.296 g in Navotas and as high as 0.475 g in Muntinlupa for 10% POE. Considering 2% POE, the average  $PA_{rock}$

values range from 0.437 g to 0.706 g, which are also in Navotas and Muntinlupa, respectively. Graphical representations of the actual values of  $PA_{rock}$  are shown as maps in Fig. 1.

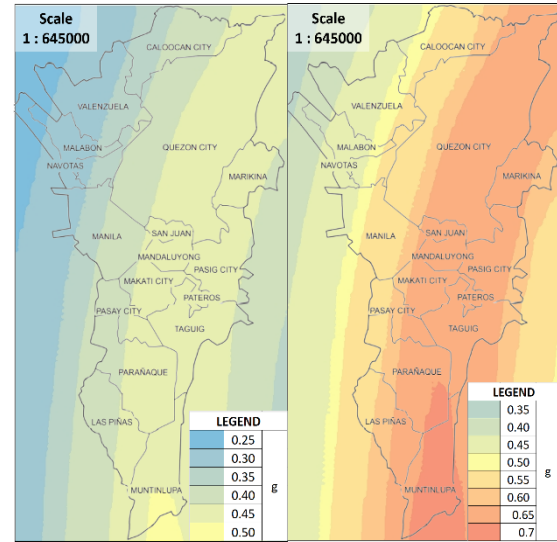


Fig. 1  $PA_{rock}$  in Metro Manila for 10% POE (left) and 2% POE (right)

As shown in the maps, the Muntinlupa area has the highest  $PA_{rock}$  values. The contour then spreads outwards, decreasing gradually as the distance from the center increases. The behavior of the contour where the highest  $PA_{rock}$  is at the center is due to the presence of the West Valley Fault, which also shows that this fault has the biggest influence on the seismic behavior in Metro Manila. The  $PA_{rock}$  values also increase as the probability of exceedance decreases, which shows that large-scale earthquakes are less common than earthquakes on a smaller scale.

##### 4.2 Shear Wave Velocity Map

A total of 1412 borehole data were collected, 1372 of which are within Metro Manila, and 40 are gathered from nearby provinces to complete the interpolation. Relating the number of data used and the area of the study area, a density of 2 borehole data for every square meter was used. Using the different geotechnical data gathered within Metro Manila, the  $V_{S30}$  in the study area were computed and mapped. Table 3 shows the summary of  $V_{S30}$  in different cities and municipalities in Metro Manila.

Based on Table 3, the average  $V_{S30}$  values in Metro Manila range from 206.48 m/s in Manila up to 554.08 m/s in Quezon City. The  $V_{S30}$  values describe the stiffness of the soil in each location, which is also attributed to the types of soil present in the area, and their corresponding SPT-N or RQD values. Fig. 2 shows the  $V_{S30}$  map of Metro Manila.

Table 3  $V_{S30}$  values within Metro Manila

Location	$V_{S30}$ (m/s)
Caloocan	451.49
Las Piñas	408.35
Makati	380.25
Malabon	260.40
Mandaluyong	546.18
Manila	206.48
Marikina	267.43
Muntinlupa	402.65
Navotas	251.78
Parañaque	498.32
Pasay	244.06
Pasig	401.75
Pateros	299.96
Quezon City	554.08
San Juan	492.20
Taguig	486.59
Valenzuela	452.02

As seen in Fig. 2, the west and east sides of Metro Manila are almost similar with low  $V_{S30}$  values, while the center is characterized by high  $V_{S30}$  values. The low values on the western side, comprised of Navotas, Malabon, Manila, and Pasay, can be attributed to the area being near the coast. The west is also mostly comprised of quarterly alluvial soil where SPT-N values are very low at the surface and are average at deeper layers [15]. Las Piñas and Parañaque are also in the west of Metro Manila, however, the  $V_{S30}$  values in the area greatly change as the area considered moves to the right.

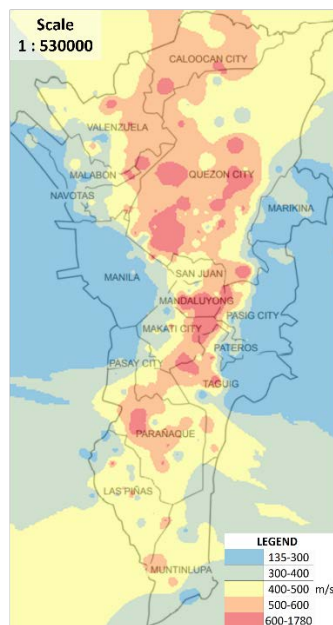


Fig. 2 Map of  $V_{S30}$  in Metro Manila

The areas in the eastern part, comprised of Marikina, Pasig, Pateros, and Taguig, have slightly higher  $V_{S30}$  values when compared to the west since the areas are far from Manila Bay. However, the soil composition in these areas is similar to the west, with almost the same SPT-N patterns.

The remaining cities in the center, which are Caloocan, Valenzuela, Quezon City, San Juan, Mandaluyong, Makati and Muntinlupa have the highest  $V_{S30}$  values. This is due to the tuff and rock formations that are common in the central part of the region [15]. With this, the SPT-N values are generally higher, and refusal can be achieved even in shallow depths.

### 4.3 Amplified Seismic Hazard Maps

Using the  $PA_{rock}$  values mapped in Fig. 1, and the  $V_{S30}$  values mapped in Fig. 2, the site amplification factors  $F_a$  and  $F_v$  were computed. To see the relationship between  $PA_{rock}$ ,  $V_{S30}$ , and the amplification factors  $F_a$  and  $F_v$ , theoretical values for the first two parameters are used to compute the amplification factors. Table 4 shows the values of  $F_a$  and  $F_v$  for increasing  $V_{S30}$  values, assuming that  $PA_{rock}$  is constant.

Table 4 Resulting amplification factors for increasing  $V_{S30}$  values

$V_{S30}$ (m/s)	$F_a$	$F_v$
150	2.737	3.405
250	2.135	2.399
350	1.813	1.905
450	1.605	1.603
550	1.456	1.397

As seen in Table 4, the values of  $F_a$  and  $F_v$  decrease as  $V_{S30}$  increases. This shows that softer soils cause stronger amplification compared to stiff soils. It can also be observed that considering the amplification factors at the highest and lowest  $V_{S30}$ , the value of  $F_a$  is 1.88 times smaller, while the value of  $F_v$  is 2.43 times smaller. This shows that  $V_{S30}$  dependency is stronger for mid-period amplification since the rate of change is greater.

On the other hand, Table 5 shows the values of  $F_a$  and  $F_v$  for increasing  $PA_{rock}$  values, assuming that  $V_{S30}$  is constant. As observed,  $F_a$  and  $F_v$  decrease as  $PA_{rock}$  increases. This is due to the nonlinearity of soil behavior [20]. When the ground accelerations are high, the soil response is governed by its high damping ratio, which results in low amplification in the soils. This shows that amplification is greater for earthquakes with low magnitudes at farther distances. Similar to Table 4, Table 5 shows that the mid-period amplification is greater than the short-period amplification.

Table 5 Resulting amplification factors for increasing  $PA_{rock}$  values

rock (g)	$F_a$	$F_v$
0.25	1.813	1.905
0.35	1.627	1.873
0.45	1.445	1.845
0.55	1.269	1.819
0.65	1.104	1.797

Comparing the amplification factors at the highest and lowest  $PA_{rock}$  values, it can be seen that  $F_a$  became 1.65 times smaller and  $F_v$  became 1.06 times smaller. This shows that short-period amplification is more dependent on the change in the  $PA_{rock}$  values. After incorporating the amplification factors into the PSHA, the amplified PGAs are computed and mapped.

Shown in Fig. 3 are the maps of amplified PGAs in Metro Manila considering the short-period amplification. Unlike the 10% POE in Fig. 1 where the contour is uniform, the contour in 10% POE in Fig. 3 is more random, with the highest accelerations at the west and east side of the region. Comparing the maps on 2% POE of Fig 1 and Fig 3, it is observed that the areas with the highest PGAs are also the areas with the lowest  $V_{S30}$ . This shows that areas with softer soils experience greater amplification. In the 2% POE of Fig 3, it is observed that the contour of the map is more similar to the contour of the non-amplified map in Fig. 1 of the same POE, where the accelerations are higher at the center, and gradually decrease as they move away.

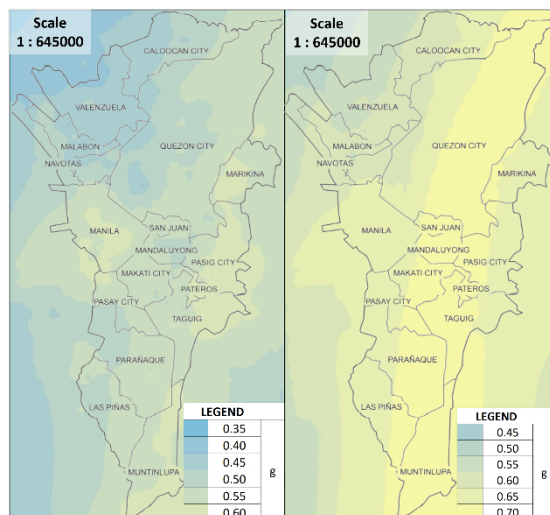


Fig. 3 Map of amplified PGAs in Metro Manila considering short-period amplification for 10% POE (left) and 2% POE (right)

The differences in the contour between the two maps in Fig 3 show how short-period amplification

is more influenced by  $PA_{rock}$  as compared to  $V_{S30}$  values. Even though some areas are shown to achieve higher PGAs due to the low  $V_{S30}$  values, the contour of the map still gradually resembles the contour of the non-amplified ones as the ground motion intensities increase and the POE decreases.

Shown in Fig. 4 are the maps of amplified PGAs in Metro Manila considering mid-period amplification. Unlike the observations in the short-period amplification where the contour tends to resemble the non-amplified maps as the POE decreases, the shape of the contour for the mid-period amplification remains the same, with only the values of the PGA increasing. The maps in Fig. 4 show that the western and eastern parts of the region have the highest PGAs. The main difference observed between the short-period and mid-period amplification is that, for the latter, the areas with the highest PGAs for 10% POE are still the same areas with the highest PGAs for 2% POE. This further shows that mid-period amplification is more dependent on  $V_{S30}$  which is constant in a certain area, regardless of the POE considered. A summary of the PGA amplifications is given in Table 6.

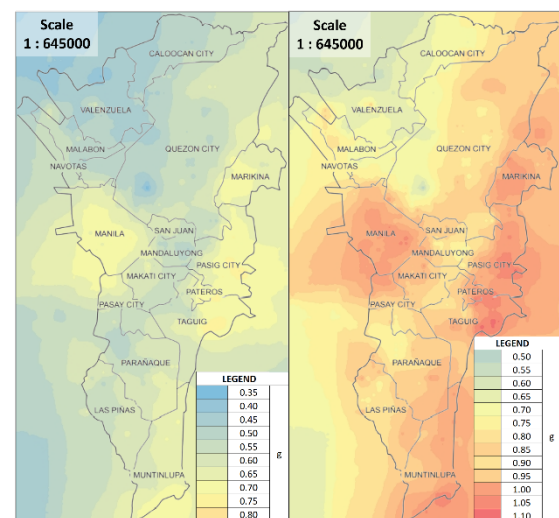


Fig. 4 Map of amplified PGAs in Metro Manila considering mid-period amplification for 10% POE (left) and 2% POE (right)

Table 6 Average of amplified PGA values in Metro Manila

Amplification	PGA (g)	
	10% POE	2% POE
Short-period	0.538	0.659
Mid-period	0.589	0.830

Table 6 summarizes the average PGA in Metro Manila for 10% and 2% POE considering short-period and mid-period amplification. As seen in the table, the average amplified PGAs can range from

0.538 g to 0.830 g depending on the probability of exceedance and period of amplification.

## 5. CONCLUSION

Due to the susceptibility of Metro Manila to seismic hazards, it is necessary to consider the possible factors, such as local soil conditions, which could intensify the damages from these hazards.

Without considering site amplification, it was observed that the center of Metro Manila has the highest  $PA_{rock}$  values, which gradually decrease as they move away from the center. On the other hand, the  $V_{S30}$  map shows that the eastern and western parts of Metro Manila exhibit low  $V_{S30}$  values due to being near a body of water and the presence of quarterly alluvial soils. The central part exhibited the highest  $V_{S30}$  values due to the presence of tuff and rock formations in the area.

After obtaining and mapping the amplified PGAs, it was seen that short-period amplification has a stronger dependency on  $PA_{rock}$ , while mid-period amplification is more dependent on  $V_{S30}$ . For short-period amplification, Metro Manila has an average PGA of 0.538 g and 0.659 g for 10% and 2% POE, respectively. Meanwhile, for mid-period amplification, the region has an average PGA of 0.589 g and 0.830 g for 10% and 2% POE, respectively.

For future studies, it is recommended to explore more methods in performing PSHA such as the use of logic trees, and more GMPEs. It would also be beneficial to use more than one correlation equation for obtaining the  $V_{S30}$  to improve the performance of these values.

## 6. ACKNOWLEDGEMENTS

The authors would like to acknowledge the Department of Science and Technology (DOST) for assisting in the funding of this study and the Philippine Institute of Volcanology and Seismology (PHIVOLCS) for providing the earthquake data used.

They would also like to thank the Department of Civil Engineering at De La Salle University, as well as the previous researchers in the same institution for sharing their knowledge and guidance throughout the conduct of this study.

## 7. REFERENCES

- [1] Monahan, P., Levson, V., McQuarrie, E., Bean, S., Henderson, P., and Sy, A., Relative Earthquake Hazard Map of Greater Victoria, Showing Areas Susceptible to Amplification of Ground Motion, Liquefaction, and Earthquake-induced Slope Instability, Geoscience Map, 2000, Ministry of Energy and Mines, British Columbia.
- [2] Navidi, S., Development of a Site Amplification Model for Use in Ground Motion Prediction Equations, The University of Texas at Austin, 2012.
- [3] Sali, A., Seismic Hazard Assessment of Metro Manila (A Foundation Engineering Analysis), Geological Society of the Philippines, 2004.
- [4] Dungca, J. and Macaraeg, C., Development of a Reference for Seismic Amplification: The Case of Metro Manila, Conference proceedings, in 19<sup>th</sup> IABSE Congress Stockholm, 2016, pp. 1015-1022.
- [5] Midorikawa, S. and Hori, A., Nonlinear Site Amplification Model Derived From Strong Motion Records Including Records of the 2011 Tohoku, Japan Earthquake, Conference proceedings, in 16<sup>th</sup> European Conference on Earthquake Engineering, 2018.
- [6] Kramer, S., Chapter 4, Geotechnical Earthquake Engineering, Prentice Hall, 1996, pp. 117-138.
- [7] Singh, S., Bazan, E. and Esteva, L., Expected Earthquake Magnitude from a Fault, Bulletin of the Seismological Society of America, Vol. 70, 1980, pp. 903-914.
- [8] Joyner, W. and Boore, D., Peak Horizontal Acceleration and Velocity from Strong Motion Records Including Records from the 1979 Imperial Valley, California Earthquake, Bulletin of the Seismological Society of America, Vol. 71, Issue 6, 1981, pp. 2011-2038.
- [9] Youngs, R., Chiou, S., Silva, W. and Humphrey, J., Strong Ground Motion Attenuation Relationships for Subduction Zone Earthquakes, Seismological Research Letters, 1997, pp. 58-73.
- [10] Marto, A., Soon, T. and Kasim, F., A Correlation of Shear Wave Velocity and Standard Penetration Resistance, Electronic Journal of Geotechnical Engineering, Vol. 18, 2013, pp. 463-471.
- [11] Hunt, R., Geotechnical Engineering Investigation Manual, Mc Graw Hill Book Co., 1984.
- [12] Ahmad, I., Hashash, Y., Khan, A. and Waseem, M., Site Amplification Factor at Mardan, Journal of Himalayan Earth Sciences, Vol. 44, Issue 2, 2011, pp. 61-70.
- [13] Boore, D., Thompson, E. and Cadet, H., Regional Correlations of  $V_{S30}$  and Velocities Averaged Over Depths Less Than and Greater Than 30 m, Bulletin of the Seismological Society of America, Vol. 101, Issue 6, 2011, pp. 3046-3059.
- [14] Dungca, J., Gozum, N., Telan, J. and Torres, V., Deep Foundation Reference for Metro Manila, Philippines, International Journal of GEOMATE, Vol. 14, Issue 45, 2018, pp. 16-21.

- [15] Dungca, J., Concepcion, I., Limyuen, M., See, T. and Vicencio, M., Soil Bearing Capacity Reference for Metro Manila, Philippines, *International Journal of GEOMATE*, Vol. 12, Issue 32, 2017, pp. 5-11.
- [16] Dungca, J., Pua, R., Que, R., Sangalang, A. and Tan, A., Mat Foundation Design Reference for Metro Manila, Philippines, *International Journal of GEOMATE*, Vol. 15, Issue 47, 2018, pp. 42-47.
- [17] Dungca, J. and Chua, R., Development of a Probabilistic Liquefaction Potential Map for Metro Manila, *International Journal of GEOMATE*, Vol. 10, Issue 2, 2016, pp. 1804-1809
- [18] Dungca, J., A Reference for the Allowable Soil Bearing Capacities in Quezon City, Philippines, *International Journal of GEOMATE*, Vol. 19, Issue 71, 2020, pp. 42-47.
- [19] Galupino, J., Garciano, L., Paringit, M. and Dungca, J., Location Based Prioritization of Surigao Municipalities Using Probabilistic Seismic Hazard Analysis (PSHA) and Geographic Information System (GIS), Conference proceedings, in *HNICEM 2019 – 9<sup>th</sup> International Conference on Humanoid, Nanotechnology, Information Technology, Communication and Control, Environment and Management*, 2017.
- [20] Kumar, A., Harinarayan, N. and Baro, O., High Amplification Factor for Low Amplitude Ground Motion: Assessment for Delhi, *Disaster Advances*, Vol. 8, Issue 12, 2015, pp. 1-11.
- 
- Copyright © Int. J. of GEOMATE All rights reserved, including making copies unless permission is obtained from the copyright proprietors.
-